Analysis of Aftershock Migration Following the 2022 Ferndale Sequence

Max Liu[1]; Saeed Mohanna[1]; Lingsen Meng[1]; Roland Bürgmann[2]

[1]University of California, Los Angeles, USA; [2]University of California, Berkeley, USA

Contact: Saeed Mohanna (saeedmohanna@g.ucla.edu)

Abstract

The 2022 M_w 6.4 Ferndale earthquake ruptured a geometrically complex region near the Mendocino Triple Junction. The Northern California Seismic Network's (NCSN) double difference catalog shows that the seismicity follows an orientation that does not align with onshore surface traces of mapped faults. We applied the EdgePhase multi-station phase picking algorithm to one month of continuous data following the mainshock, intending to investigate fault geometry and seismicity migration during the aftershock sequence. We use software (REAL, HypoInverse, HypoDD, GrowClust) within the LOC-FLOW algorithm to perform the phase association and event relocation. In our updated catalog, we detect 9.5 times more events than the local catalog, with an 82% match to the events found by NCSN. Analysis of the spatiotemporal evolution of seismicity along the strike and dip directions of the USGS finite fault inversion result reveals that pore fluid diffusion (which follows a $\sqrt{t}$ relation) may have played a role in aftershock production in this sequence. We will explore other possible migration mechanisms, such as rate-and-state friction, and analyze geodetic data to look for indications of afterslip. Comparing the 3-D locations of the events with the location of the Gorda plate geometry in addition to the orientations of focal mechanism nodal planes with offshore faults, we find that the mainshock likely occurred within the Gorda plate with aftershocks migrating down-dip in the subducting slab.

Data and Methodology

We collected data for one month following the mainshock from 30 velocity and accelerometer stations, spanning 4 different networks within 1° of the USGS hypocenter of the M_w 6.4 event. Phases were picked using our group's multi-station phase-picking algorithm called EdgePhase (Feng et al., 2022). EdgePhase was trained using waveforms from the year 2021 in the Southern California Seismic Network's dataset. Using detection thresholds of 0.12 and 0.15, we detected 406,820 and 284,969 P- and S-phases, respectively.

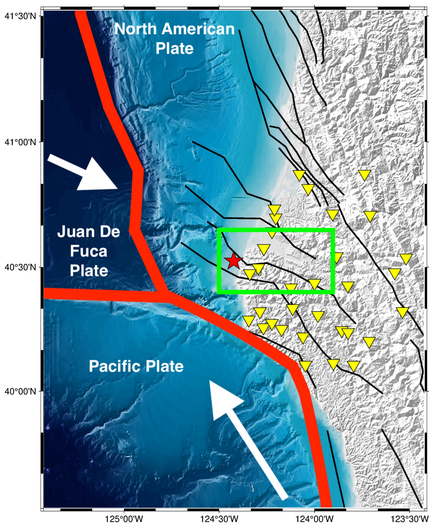

Using the LOC-FLOW workflow (Zhang et al., 2022) for locating earthquakes, phases were associated with the Rapid Earthquake Association and Location (REAL) algorithm. Absolute and relative earthquake locations were then obtained using the HypoInverse, HypoDD, and GrowClust algorithms. Due to the complex velocity structure of the region, we utilized HypoInverse's ability to accommodate the multiple velocity models used in NCSN's location method. For software that could only accommodate one velocity model, we averaged two velocity models that defined the region containing all 30 stations.

Figure 1: Map showing all the stations used (yellow inverted triangles), nearby plate boundaries (thick red lines) and motions (white arrows), the location of the mainshock (red star), surface traces of nearby faults (black lines, Shen et al.; 2022) and our area of study (green box) shown in figure 3.

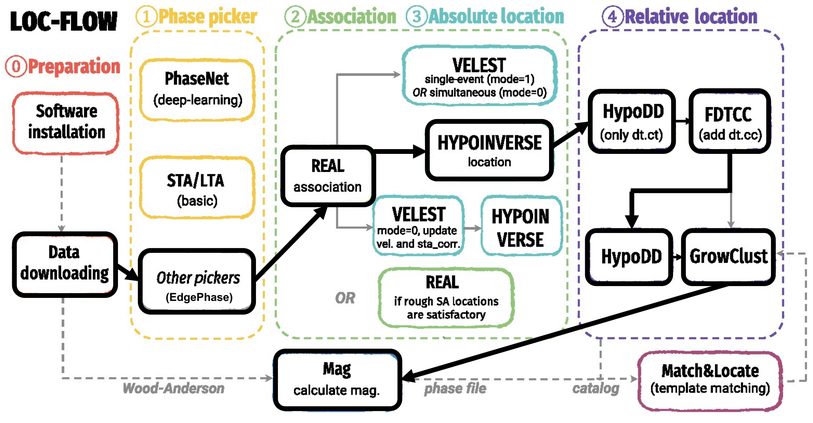

Figure 2: Modified version of the LOC-FLOW algorithm outline from Zhang et al. (2022) with the steps we use highlighted by the black borders and arrowheads.

Results

Our event locations mostly align with those of the Northern California Seismic Network (NCSN), with an 82% match ($\Delta t = 3$ s, $\Delta s = 3$ km) to those events in NCSN. We detected 2821 more events than NCSN, leading to a lower magnitude of completeness (M_c=1.7 compared to NCSN's 2.1) estimated by the b-value stability method using the SEDA software (Lombardi, 2017; Figure 4).

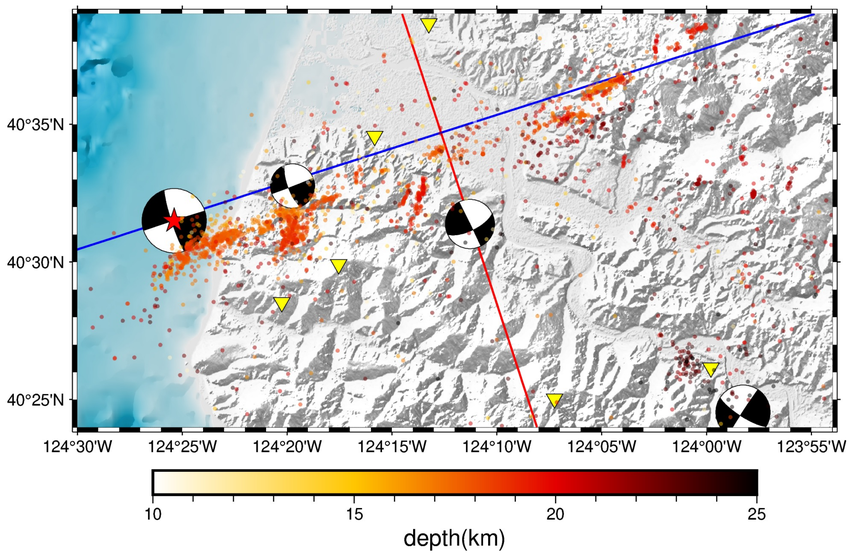

Figure 3: Map showing our aftershock locations color-coded by time after the mainshock. The blue and red lines show the strike and strike-normal of the fault plane used in Dreger's (2023) obtained slip model, respectively. The red star shows the USGS hypocenter of the M_w 6.4 mainshock. Focal mechanisms of the mainshock and large aftershocks are plotted.

The seismicity does not follow the orientation of nearby mapped surface fault traces. When plotting the depth of the seismicity (Figure 3), we find that it is likely that most of the events occurred within the subducting Gorda plate. This is further supported by the orientations of several aftershock focal mechanisms (Figure 2) aligning with those of the offshore surface fault traces.

The slip model obtained by Dreger (2023) places the main coseismic slip patch at a deeper depth than that of the USGS finite fault solution. Our obtained seismicity aligns with this patch well. Throughout the aftershock sequence, there is evidence of migration downdip within the subducting Gorda plate.

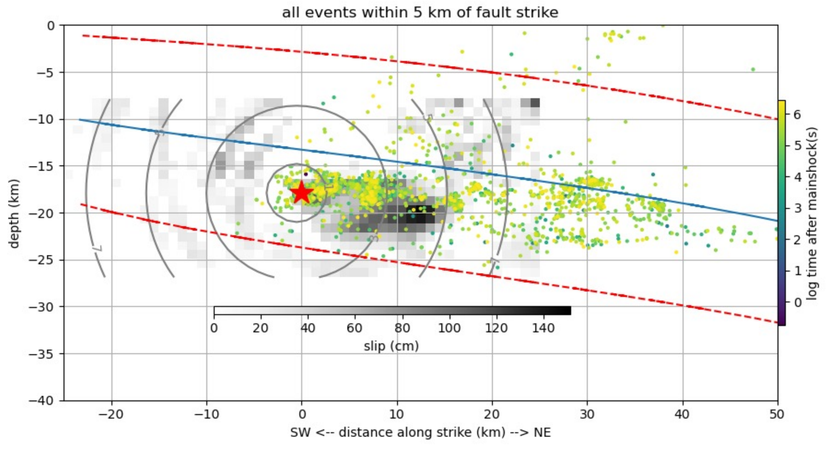

Figure 3: Slip model (Dreger, 2023) with projected aftershock locations and the Slab 2.0 (Hayes, 2018) interface (blue line) with uncertainties (red-dashed lines) onto the finite fault plane. Grey contours show rupture front at 2-s intervals beginning at 1s after the mainshock.

Acknowledgements

This research was funded by the National Science Foundation's CAREER EAR-1848486 grant and the John W. West Fund. We thank Dr. Kathryn Materna for valuable discussions on post-seismic slip. We thank Dr. Doug Dreger for providing us with their obtained slip model for the M6.4 event.

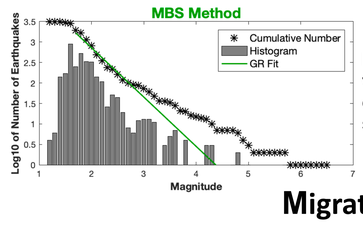

Figure 4: Graph showing the result of applying the b-value stability method to estimate the magnitude of completeness of our catalog using the SEDA software (Lombardi, 2017)

Migration analysis

We also detect a cluster of seismicity towards the southeast of the finite fault plane. To understand the migration mechanisms driving this aftershock sequence, we project events onto red and blue lines from Figure 2 if they are located within 20 and 5 km of them, respectively. We then fit diffusivity relations to the results. We found that diffusivity values ranging between 0.06-0.8 m²/s fit the data well.

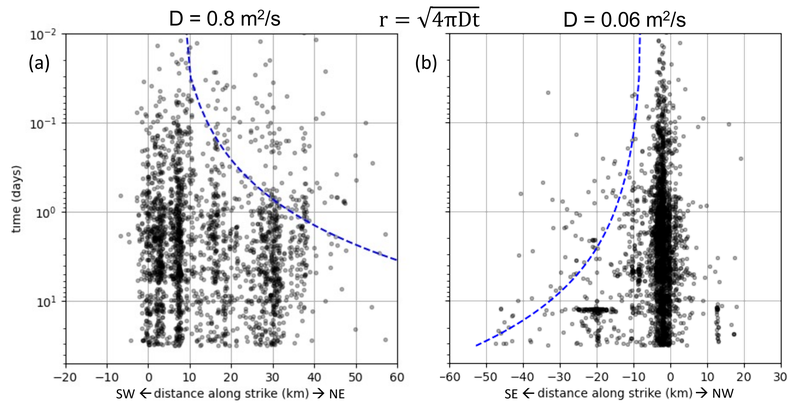

Figure 5: Spatiotemporal evolution of aftershocks (black dots) along (a) the strike and (b) strike-normal of the finite fault plane. Pore fluid diffusion relations are plotted as dashed lines in both figures.

Key takeaways

1. Using a multi-station phase picking algorithm and a popular earthquake location workflow, we detect 9.5 times more events than the local catalog.
2. By examining the distribution of seismicity and orientation of focal mechanisms, we found that it is likely that most aftershocks occurred within the subducting Gorda plate.
3. Spatiotemporal evolution analysis suggests an apparent expansion of seismicity that follows a $\sqrt{t}$ relation, which suggests that pore fluid diffusion is driving these aftershocks. Depending on the direction we project onto, we see that diffusivity values ranging between 0.06-0.8 m²/s lead to good fits to the data. Typical crustal diffusivity values for tectonic earthquakes are in the range 0.01-1 m²/s (Chen et al., 2012) so these values are reasonable.
4. We need to consider other mechanisms that may have contributed to the migration of this sequence, such as afterslip and rate-and-state friction. Though afterslip does not appear to be a contributor in Figure 5, examining data recorded at nearby GPS stations to look for signals of post-seismic deformation would be beneficial in deciding to rule out that mechanism.

References

Chen, X., P. M. Shearer, and R. E. Abercrombie (2012), Spatial migration of earthquakes within seismic clusters in Southern California: Evidence for fluid diffusion, *J. Geophys. Res.*, **117**, B04301, doi:10.1029/2011JB008973.

Dreger, D., written communication (2023).

Feng, T., Mohanna, S., & Meng, L. (2022). EdgePhase: A deep learning model for multi-station seismic phase picking. Geochemistry, Geophysics, Geosystems, 23, e2022GC010453. https://doi.org/10.1029/2022GC010453

Hayes, G., 2018, Slab2 - A Comprehensive Subduction Zone Geometry Model: U.S. Geological Survey data release, https://doi.org/10.5066/F7PV6JNV.

Lombardi, A. M. (2017). SEDA: a software package for the statistical earthquake data analysis. Scientific Reports, 7(1). https://doi.org/10.1038/srep44171

Zhang M., M. Liu, T. Feng, R. Wang, and W. Zhu. LOC-FLOW: An End-to-End Machine-Learning-Based High-Precision Earthquake Location Workflow, Seismol. Res. Lett., 2022, doi: 10.1785/0220220019.

Zheng-Kang Shen, Peter Bird; NeoKinema Deformation Model for the 2023 Update to the U.S. National Seismic Hazard Model. *Seismological Research Letters* 2022;; 93 (6): 3037–3052. doi: https://doi.org/10.1785/0220220179